



Phenotyping heart failure by echocardiography: Imaging of ventricular function and haemodynamics at rest and exercise

Otto A Smiseth, Erwan Donal, Espen Boe, Jong-Won Ha, Joao F Fernandes, Pablo Lamata

► To cite this version:

Otto A Smiseth, Erwan Donal, Espen Boe, Jong-Won Ha, Joao F Fernandes, et al.. Phenotyping heart failure by echocardiography: Imaging of ventricular function and haemodynamics at rest and exercise. European Heart Journal - Cardiovascular Imaging, 2023, <10.1093/ehjci/jead196>. <hal-04196124>

HAL Id: hal-04196124

<https://hal.science/hal-04196124v1>

Submitted on 5 Sep 2023

HAL is a multi-disciplinary open access archive for the deposit and dissemination of scientific research documents, whether they are published or not. The documents may come from teaching and research institutions in France or abroad, or from public or private research centers.

L'archive ouverte pluridisciplinaire **HAL**, est destinée au dépôt et à la diffusion de documents scientifiques de niveau recherche, publiés ou non, émanant des établissements d'enseignement et de recherche français ou étrangers, des laboratoires publics ou privés.



Distributed under a Creative Commons CC BY-NC 4.0 - Attribution - Non-commercial use - International License

Phenotyping heart failure by echocardiography: imaging of ventricular function and haemodynamics at rest and exercise

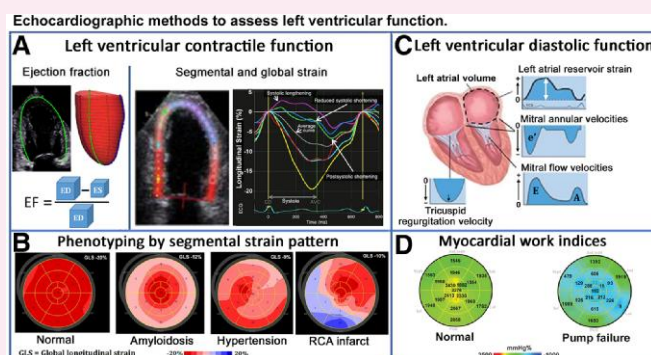
Otto A. Smiseth ^{1*}, Erwan Donal ², Espen Boe ³, Jong-Won Ha ⁴, Joao F. Fernandes ⁵, and Pablo Lamata ⁵

¹Division of Cardiovascular and Pulmonary Diseases, Institute for Surgical Research, Oslo University Hospital and University of Oslo, Oslo, Norway; ²Department of Cardiology, CHU Rennes and Inserm, LTSI, University of Rennes, Rennes, France; ³Department of Cardiology, Oslo University Hospital, Rikshospitalet, Sognsvannsveien 20, Oslo, Norway; ⁴Department of Internal Medicine, Yonsei University College of Medicine, Seoul, South Korea; and ⁵Department of Biomedical Engineering, School of Biomedical Engineering and Imaging Sciences, King's College London, London, UK

Received 19 June 2023; accepted after revision 20 June 2023; online publish-ahead-of-print 5 August 2023

Traditionally, congestive heart failure (HF) was phenotyped by echocardiography or other imaging techniques according to left ventricular (LV) ejection fraction (LVEF). The more recent echocardiographic modality speckle tracking strain is complementary to LVEF, as it is more sensitive to diagnose mild systolic dysfunction. Furthermore, when LV systolic dysfunction is associated with a small, hypertrophic ventricle, EF is often normal or supernormal, whereas LV global longitudinal strain can reveal reduced contractility. In addition, segmental strain patterns may be used to identify specific cardiomyopathies, which in some cases can be treated with patient-specific medicine. In HF with preserved EF (HFpEF), a diagnostic hallmark is elevated LV filling pressure, which can be diagnosed with good accuracy by applying a set of echocardiographic parameters. Patients with HFpEF often have normal filling pressure at rest, and a non-invasive or invasive diastolic stress test may be used to identify abnormal elevation of filling pressure during exercise. The novel parameter LV work index, which incorporates afterload, is a promising tool for quantification of LV contractile function and efficiency. Another novel modality is shear wave imaging for diagnosing stiff ventricles, but clinical utility remains to be determined. In conclusion, echocardiographic imaging of cardiac function should include LV strain as a supplementary method to LVEF. Echocardiographic parameters can identify elevated LV filling pressure with good accuracy and may be applied in the diagnostic workup of patients suspected of HFpEF.

Graphical Abstract



(A) Calculation of ejection fraction and strain. (B) Systolic strain pattern for different phenotypes. RCA, right coronary artery. (C) Parameters of diastolic function. (D) Myocardial work index by echocardiography. Adapted from Chan et al.²²

* Corresponding author. E-mail: otto.smiseth@gmail.com

© The Author(s) 2023. Published by Oxford University Press on behalf of the European Society of Cardiology.

This is an Open Access article distributed under the terms of the Creative Commons Attribution-NonCommercial License (<https://creativecommons.org/licenses/by-nc/4.0/>), which permits non-commercial re-use, distribution, and reproduction in any medium, provided the original work is properly cited. For commercial re-use, please contact journals.permissions@oup.com

echocardiography • heart failure • diastolic function • digital twin • left ventricular ejection fraction • strain imaging • systolic function

- Myocardial strain imaging by speckle tracking echocardiography is complementary to ejection fraction (EF) and should be done when EF is normal in patients suspected heart failure (HF).
- Global longitudinal strain (GLS) is more sensitive than EF to diagnose mild systolic dysfunction.
- In hearts with a small, hypertrophic ventricle, EF is often normal or supernormal, whereas GLS can reveal reduced contractility.
- Several cardiomyopathies can be diagnosed by characteristic distribution patterns of left ventricular (LV) segmental strains.
- In patients suspected of HF, echocardiography can identify elevated LV filling pressure with good accuracy.
- When LV filling pressure is normal at rest, a diastolic stress test may be needed to confirm the HF diagnosis.
- Future development of digital twin technology is expected to facilitate understanding of complex interactions between different biological processes in the failing heart.

Heart failure (HF) is a highly prevalent condition that is associated with significant morbidity and a poor prognosis. Since the 1980s, HF phenotyping was based mainly on clinical symptoms and signs and on measurement of left ventricular (LV) ejection fraction (LVEF). This categorization was proved successful in HF with reduced EF (HFrEF), as reflected in improved life quality and reduced mortality in response to drugs and devices in this phenotype.¹

Better insights into the pathophysiology of HF, advances in cardiac imaging, and introduction of therapies targeting specific cardiomyopathies have stimulated implementation of personalized medicine in management of patients with HF. Rather than applying a traditional approach and assuming that ‘one size fits all’, today, many patients can receive personalized therapies based on more refined phenotyping.

Echocardiography plays a cardinal role in establishing the presence of a cardiac abnormality and in defining specific aetiology of HF. As reviewed in separate state-of-the-art articles in this issue of the journal, other imaging modalities and genetic testing often provide diagnostic information that is complementary to echocardiography. The present article addresses how echocardiography may be applied to improve phenotyping by imaging ventricular function. This article also presents haemodynamic correlates to imaging data to better understand which features of cardiovascular function are reflected in the different phenotypes.

HF is a clinical syndrome with different aetiologies and diverse pathophysiology rather than a specific disease. Mechanistically, the problem of a failing heart is inability to pump enough blood to meet the body's need for oxygen and nutrients.² Limited supply of oxygen to the body causes symptoms of fatigue and exercise intolerance ('forward failure'). Furthermore, as a compensatory mechanism to maintain stroke volume by the Frank-Starling mechanism, there is elevation of LV filling

Due to the complexity of the disorder and the diversity of the pathophysiology, it has been challenging to agree upon a unified definition of HF. Recently, an international consensus on its definition was obtained among several medical organizations working with HF. They proposed that HF was defined as a clinical syndrome with symptoms and/or signs caused by a structural and/or functional cardiac abnormality corroborated by elevated natriuretic peptide levels and/or objective evidence of pulmonary or systemic congestion.³

Systolic function refers to the heart's ability to generate force by contraction to eject blood into the aorta. LV pressure–volume analysis is the gold standard for quantifying LV systolic function but requires invasive measurements combined with a loading intervention and is therefore rarely used in clinical settings. Instead, echocardiography is used as the standard method for quantification of LV function in daily clinical work.

LVEF is calculated as stroke volume indexed to end-diastolic volume (EDV) and is used successfully to phenotype and identify patients who need HF therapy. This conventional phenotyping includes the following groups: HFrEF ($\leq 40\%$), HF with mildly reduced EF (HFmrEF) ($41\text{--}49\%$), and HF with preserved EF (HFpEF) ($\geq 50\%$).¹ There are, however, several limitations of this simplified phenotyping, which are discussed subsequently. First, LVEF has relatively low sensitivity to identify mild systolic dysfunction as detected by strain metrics. Therefore, patients with HFpEF often have systolic dysfunction, as reflected in reduced LV longitudinal shortening. This is illustrated in *Figure 1*, which shows that HFpEF patients with EF $> 50\%$ have lower values for LV global longitudinal strain (GLS) than normal controls, consistent with mild systolic dysfunction.

Second, LVEF has limited ability to serve as a prognostic indicator. This is illustrated *Figure 2A*, which is from a large HF study that compared prognosis in patients according to LVEF. It was found that 5-year mortality was similar in patients with $EF \geq 50\%$, $\leq 40\%$, and 41–49%. These observations are supported by previous studies that have compared mortality in HFrEF and HFpEF.⁵

The use of LVEF as a prognostic indicator is further complicated by a U-shaped relationship between EF and cardiovascular risk, as shown in *Figure 2B*. It is not clear why supernormal EF is associated with high risk but may, in part, be caused by a confounding risk marker, such as LV hypertrophy, which tends to cause small LV cavity volumes. Further studies should explore if the U-shaped association between risk and circumferential LV strain illustrated in *Figure 2C* reflects a similar phenomenon. Potentially, increased circumferential strain is a compensatory mechanism that maintains EF in the early phase of HF when GLS is mildly reduced.⁷

The data in *Figure 2D* are from a combined clinical and modelling study, which showed a much flatter slope for GLS vs. EF than for circumferential strain vs. EF.⁸ This would imply that EF is less sensitive

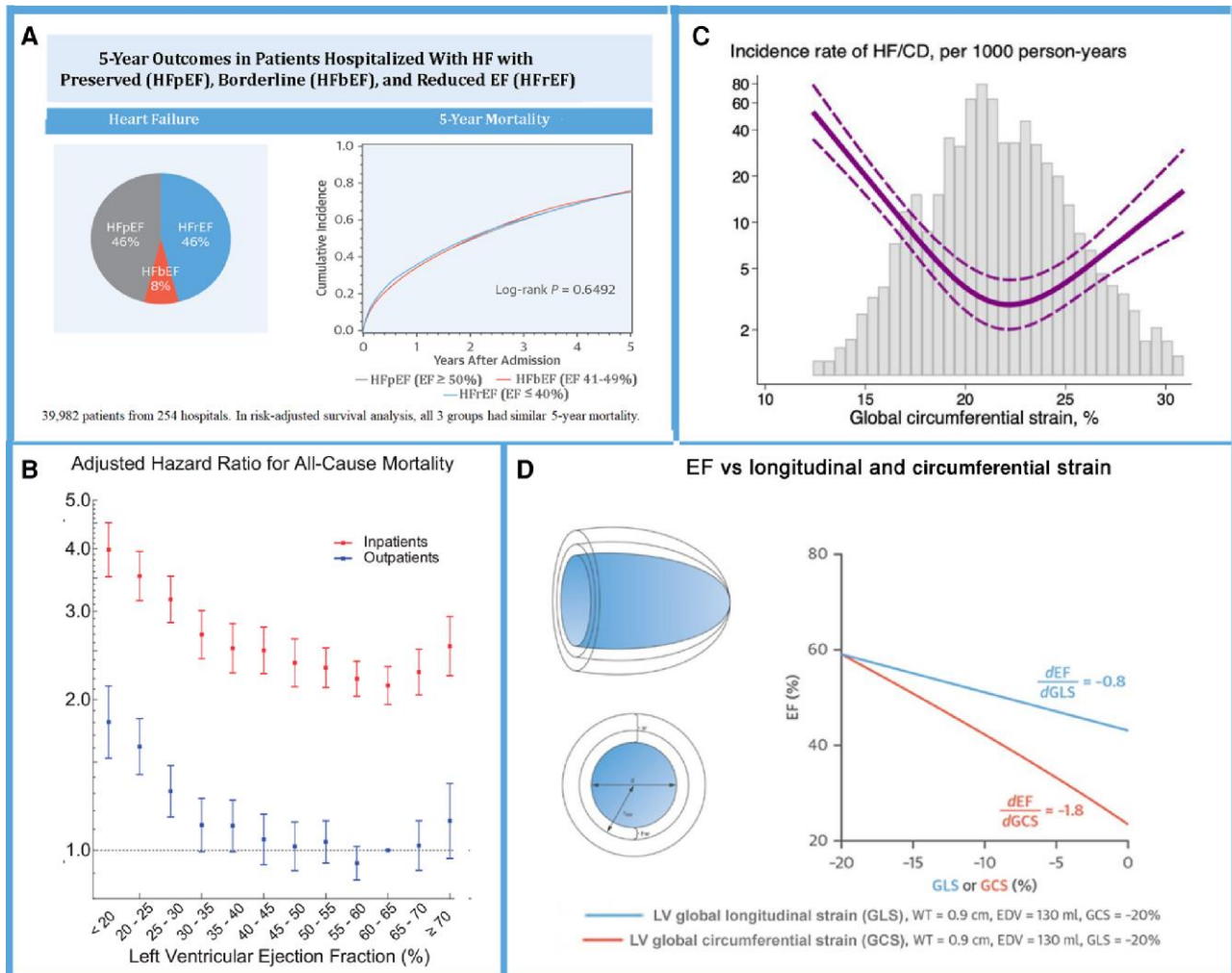


Figure 2 EF as a prognostic indicator: (A) 5-year mortality was similar in HF patients with preserved, borderline, and reduced LVEF. Modified from Shah et al.⁵ (B) A U-shaped relationship was observed between LVEF and adjusted hazard ratios in patients with HF (number of echocardiograms = 40 616). Error bars, 95% confidence interval.⁶ (C) A U-shaped relationship was observed between LV GCS and the incidence rate of HF and/or CD (2874 patients).⁷ (D) Relationships between EF and LV strains, showing a much flatter slope for GLS vs. EF than for GCS vs. EF. CD, cardiovascular death; EF, ejection fraction; GCS, global circumferential strain; GLS, global longitudinal strain. EDV, end-diastolic volume; WT, wall thickness. Adapted from Stokke et al.⁸

As suggested by recent data from a large retrospective study of a general population, elevated GCS was independently associated with a higher risk of HF/cardiac death when LVEF was above 50% (Figure 2C).⁷ These observations, suggesting a role for measuring LV GCS clinically, need to be tested in future prospective studies.

Measurement of radial strain by STE is challenging because fewer speckles are present, and similar to circumferential strain, radial strains increase markedly from the outer to the inner layers of the LV wall due to a geometrical effect. There is also a transmural gradient for longitudinal strain, but it is much smaller than for circumferential and radial strains due to a larger radius of curvature in the long axis.¹⁶

Strain imaging may also be used to measure LV twist and torsion, but so far, this application has been limited to research studies.¹⁷ The strain rate is another parameter that is feasible by STE but has so far not been implemented in clinical routine.

As explained in this section, myocardial strain imaging is a useful supplement to EF in HF diagnostics. Measurement of GLS should be

considered in every patient who is evaluated for potential systolic dysfunction. For diagnosing specific cardiomyopathies, LV strain provides valuable diagnostic information that cannot be obtained by measuring EF or by visual assessment of contractile function. In addition, GLS is a strong prognostic marker.

Other parameters of systolic function

Cardiac output is an important parameter of systolic function, which is expressed as the amount of blood pumped out in the aorta per time unit. Cardiac output can be measured using the Doppler velocity–time integral combined with the LV outflow tract diameter to measure stroke volume, which is then multiplied by the heart rate. Peak systolic mitral annular velocity (s') using tissue Doppler and mitral annular plane

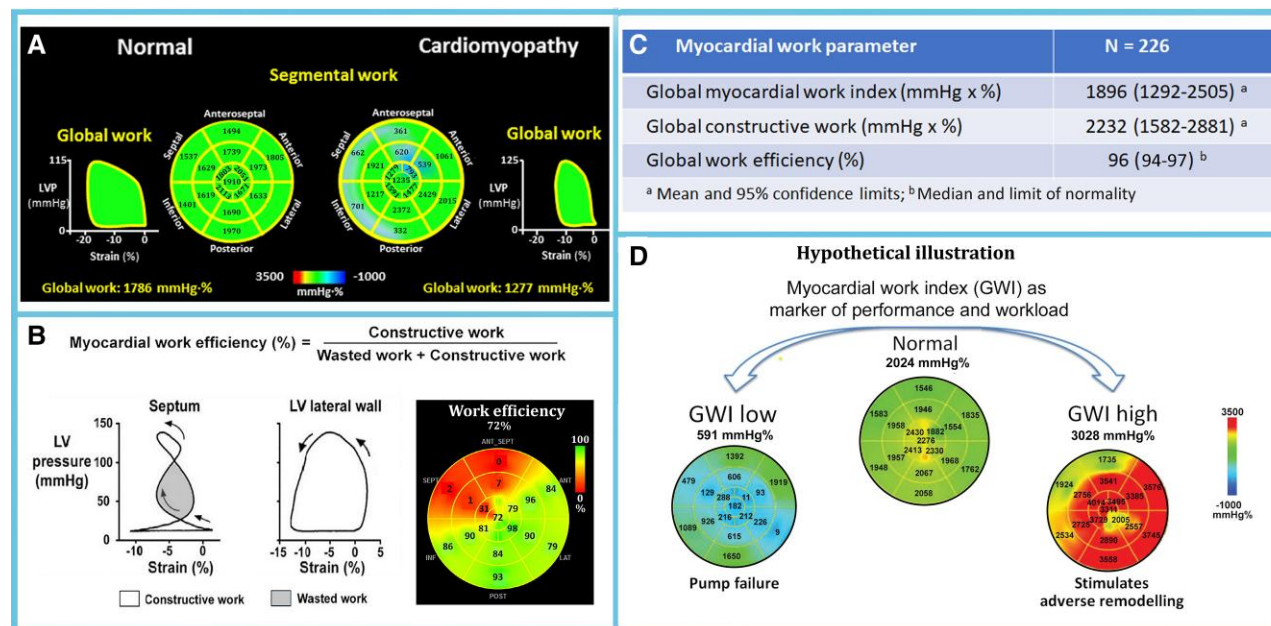


Figure 3 (A) Calculation of MWV indices in a normal subject and in a patient with cardiomyopathy.²⁰ (B) Measurements in a patient with congestive HF and left bundle branch block. The formula for calculation of MWV efficiency (WE) is shown. There is low WE in the septum due to substantial wasted work (WW) and therefore low global WE, as shown in the bull's eye plot. Arrows indicate the direction of rotation of pressure-strain coordinates. (C) Reference ranges for normal MW indices.²¹ (D) Hypothetical illustration suggesting how the echocardiographic MW index may be used as an indicator of pump function and to reflect myocardial workload as a stimulus to adverse remodelling. Data adapted from Chan *et al.*²² showing a patient with non-ischaemic cardiomyopathy (left), one with hypertension (right), and a normal subject (centre).

systolic excursion (MAPSE) using M-mode are useful alternatives to LVEF and strain in patients with poor image quality.¹⁸

Myocardial work and efficiency

Myocardial work (MW) is a recent non-invasive modality that combines LV strain with a non-invasive estimate of LV pressure via cuff blood pressure.¹⁹ It includes a tool that shows the pressure–strain curves. Since MW indices incorporate systolic pressure, these parameters may be applied during changes in afterload. Furthermore, whereas GLS provides a measure at only one time point during the heart cycle, work utilizes strain values from the entire systole from onset contraction until onset of LV filling (Figure 3A). In addition, this modality includes a measure of efficiency and therefore provides more comprehensive data on LV function than by just measuring strain. Furthermore, regional differences in MW correlate with regional myocardial glucose metabolism, evaluated using positron emission tomography (PET) imaging.¹⁹

The MW index is calculated by differentiation of the strain curve and multiplying it with instantaneous LV pressure. This product is a measure of instantaneous power, which is integrated over time from mitral valve closure to mitral valve opening and gives segmental and global MW.²³ Alternatively, MW can also be calculated as the area of the LV pressure-strain loop.¹⁹ Importantly, these estimates of work use pressure as a surrogate for force, use relative dimension, and do not incorporate radii of curvature. Furthermore, the LV pressure estimate does not take into consideration individual differences in LV diastolic pressure. These limitations should be kept in mind when interpreting MW indices.

The LV global work index (GWI) is calculated as an average of segmental values. As illustrated in *Figure 3*, several different work indices may be calculated. Constructive work (CW) is defined as work that contributes

to global LV pump function and is measured as work during segmental shortening. In dysfunctional ventricles, there may be segments that lengthen in systole, and the work performed on these segments by other parts of the ventricle represents a waste of energy. Calculation of wasted work (WW) is illustrated in *Figure 3B*. Myocardial shortening during LV isovolumic relaxation (post-systolic shortening) is also considered a waste of energy. As illustrated in *Figure 3*, work efficiency (WE) is calculated as CW divided by the sum of CW and WW.

Approximate normal values of the indices of work are as follows: GWI 1900 mmHg%, global CW 2200 mmHg%, and global WE 96% (Figure 3C). The GWI is slightly higher in women than in men, and it increases with age.

The MW index based on LV pressure–strain analysis measures global as well as segmental work, which may be of importance to localize segments with impaired performance, and in some disorders, it may be important to identify segments with abnormally high workload or asymmetry in workload, as illustrated in [Figure 3B and D](#).

Studies of the clinical value of MW indices have been published in the field of cardio-oncology²⁴ and in patients who are candidates for cardiac resynchronization therapy.²⁵ There are also promising data on application of MW indices in the evaluation of patients with ischaemic heart diseases or valvular heart diseases. The clinical demonstration of its value remains a matter of large prospective studies. The 'tool' remains young and is a very promising less load-dependent method for assessing LV systolic function.

Cardiac power

Cardiac power is a measure of cardiac performance that integrates pressure (afterload), flow, and heart rate and expresses the energy

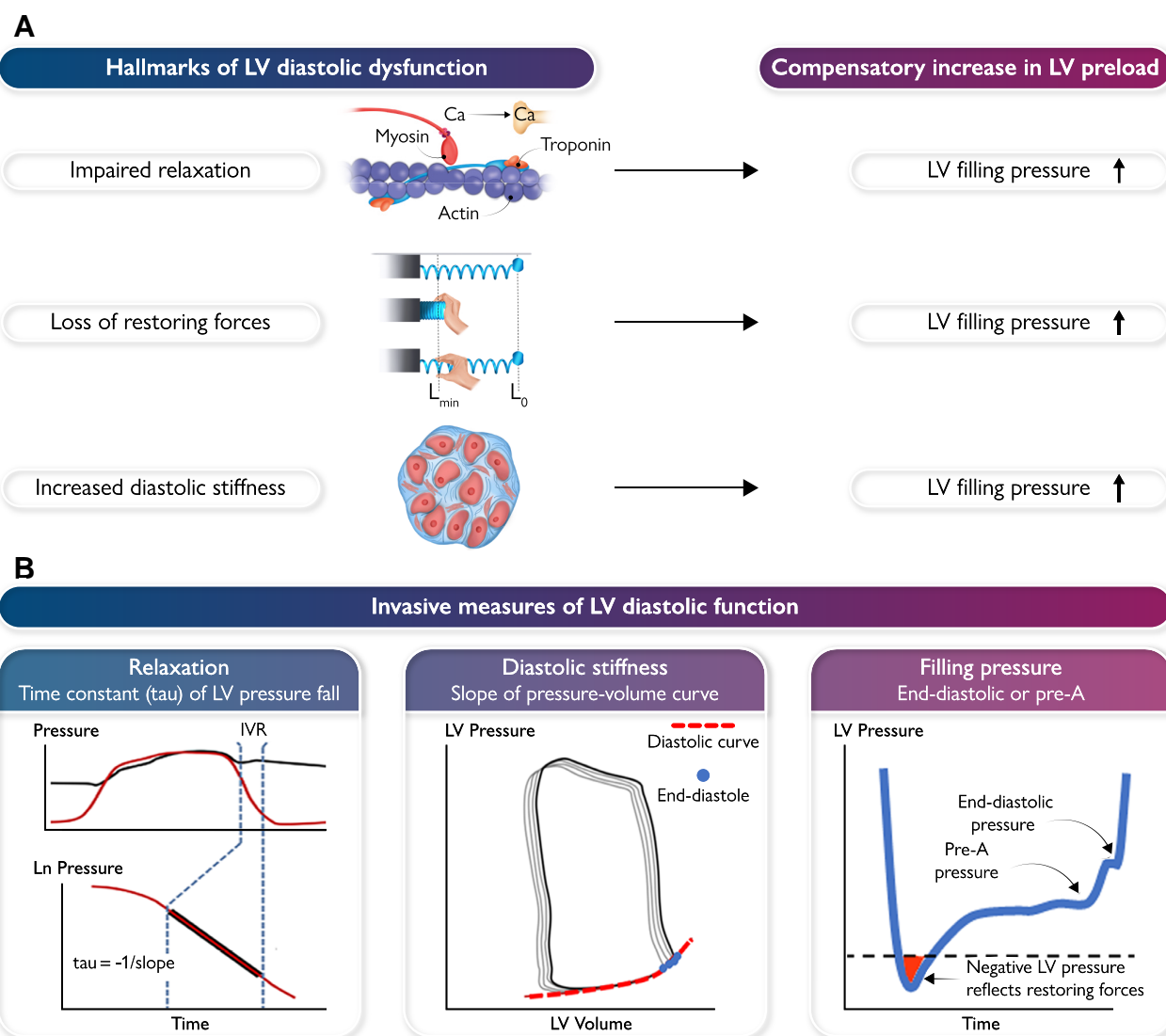


Figure 4 (A) The three fundamental mechanisms of LV diastolic dysfunction are impaired myocardial relaxation, loss of restoring forces, and increased passive elastic stiffness. Each one of these mechanisms may impair LV filling, and as a compensatory mechanism, there is elevated LV filling pressure. Based on Opdahl et al.²⁷ L_{\min} , minimum length of the compressed spring; L_0 , unstressed length. (B) Illustration of invasive methods for measuring diastolic function. The left panel shows calculation of the time constant of LV isovolumic pressure fall (τ).²⁸ The middle panel shows LV diastolic stiffness calculated as the slope of the diastolic PV curve. The right panel shows the measurement of LV filling pressure.

During congestive HF (right panel), there was loss of diastolic suction, as indicated by elevated minimum LV pressure, and increased trans-mitral flow during exercise was attributed to a marked increase in LA pressure. Figure 7B shows data from two patients, one with slightly negative LV early diastolic pressures during exercise and one with marked elevation of early and late diastolic pressures, indicating diastolic dysfunction.

A non-invasive diastolic stress test with measurement of E/e' and peak TR velocity as markers of LV filling pressure during exercise can be added in the setting of suspected HFpEF and normal resting LV filling pressure (Figure 8A).³⁴ Candidates for the test are patients with Grade I diastolic dysfunction and signs of delayed myocardial relaxation as indicated by septal $e' < 7$ or lateral $e' < 10$ cm/s. Criteria for positive diastolic stress test are signs of elevated filling pressure, as shown in

Figure 8A. For further details of the test, it is referred to Ha et al.³⁵ In some cases, an invasive diastolic stress test may be needed for a conclusive diagnosis of HFpEF, as illustrated in Figure 8B.

The LA as a mirror of LV function

Imaging of the LA provides important diagnostic information in patients suspected of HF, as summarized in Figure 9. In the absence of atrial arrhythmias, an enlarged LA is often the result of long-standing elevation of LV filling pressure. The recommended upper normal limit for LAVi by 2D echocardiography is 34 mL/m². However, ~10% of apparently heart-healthy individuals have LAVi above 34 mL/m².⁴⁰ LA volume can also be quantified by 3D echocardiography and cardiac magnetic

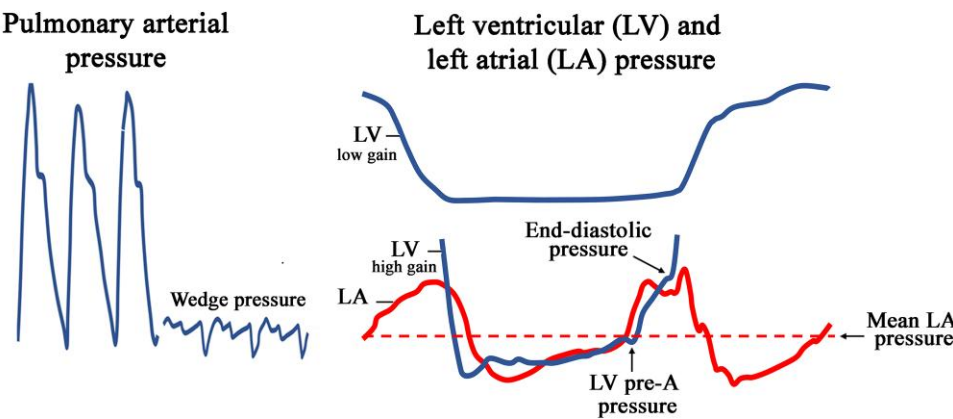
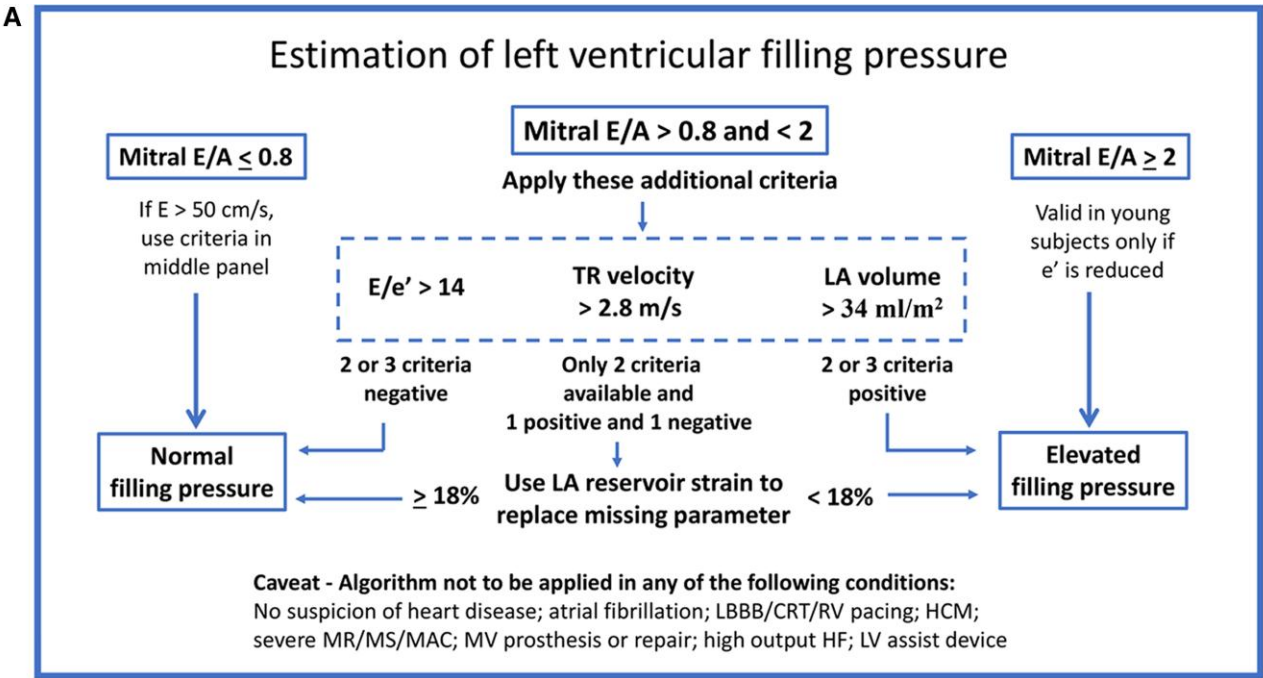


Figure 5 Definitions of LV filling pressure. The left panel shows recordings of pulmonary arterial pressure along with PCWP. The right panel shows simultaneous recordings of LV and LA pressure, and LV pre-A pressure and LVEDP are indicated. The horizontal dashed line indicates mean LA pressure.



B Criteria for normal and abnormal LV diastolic function

Parameters	Cutoffs for abnormal	
1. Septal e' or lateral e'	< 7 cm/s < 10 cm/s	Diastolic function is normal if > one half (3 of 4 or 2 of 3) of values are normal
2. Average E/e' ratio	> 14	Diastolic function is abnormal if > one half (3 of 4 or 2 of 3) of values are abnormal
3. LA volume index	> 34 ml/m ²	The study is inconclusive if 2 of 4 parameters meet cutoff criteria
4. Peak TR velocity	> 2.8 m/s	

C Criteria for grading of LV diastolic dysfunction according to filling pattern and filling pressure

	Grade I	Grade II	Grade III
Mitral flow velocities			
Mitral E/A ratio	≤ 0.8	> 0.8 to < 2	≥ 2
LV filling pressure	Normal or low	Elevated	Elevated

Figure 6 (A) Algorithm for assessing LV filling pressure by echocardiography. According to a consensus document from EACVI.³¹ LBBB, left bundle branch block; RV, right ventricular; CRT, cardiac resynchronization therapy; HCM, hypertrophic cardiomyopathy; MR, mitral regurgitation; MS, mitral stenosis; MAC, mitral annular calcification; MV, mitral valve. (B) Criteria for normal and abnormal LV diastolic function. (C) Criteria for grading of diastolic dysfunction. According to a consensus document.³¹

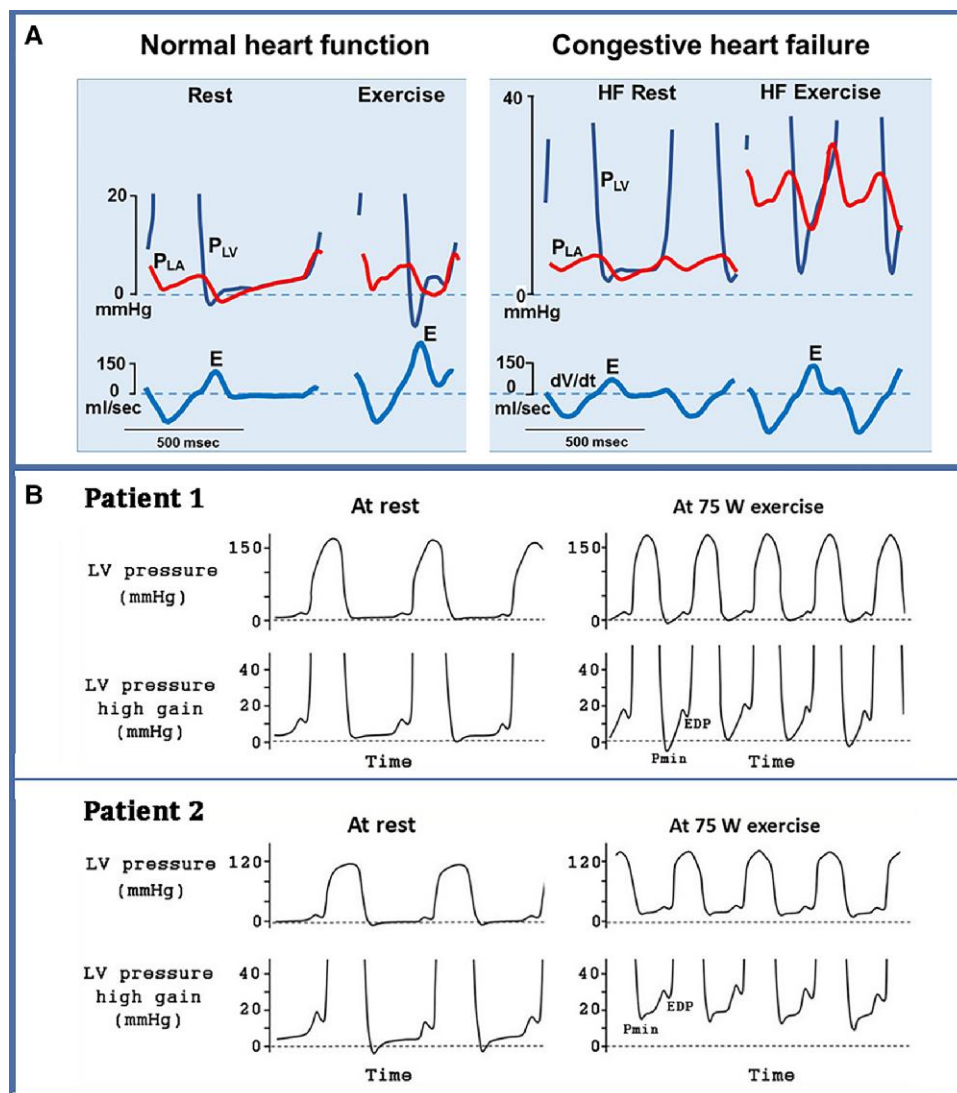


Figure 7 (A) Loss of diastolic suction in the failing heart: experimental study showing a normal heart (left panel), which generates markedly negative diastolic pressure during exercise, causing LV filling by suction. Thereby, the normal heart can increase mitral *E* with no rise in LA pressure. During HF (right panel), LV minimum pressure does not decrease during exercise and transmitral flow increases by elevation of LA pressure. Transmitral flow rate was measured as *dV/dt*. Adapted from Cheng et al.³¹ (B) Recordings from two patients 1 year after percutaneous coronary intervention but no coronary stenosis at the time of the study. Patient A responds to bicycle exercise with mild elevation of LVEDP and a fall in minimum LV pressure (*P_{min}*), indicating maintained diastolic suction. In Patient B, however, LVEDP approaches 30 mmHg during exercise and there is a marked elevation of minimum LV pressure, indicating loss of diastolic suction. To maintain LV filling during exercise, Patient B would require marked elevation of LA pressure. Adapted from Hong et al.³³

resonance (CMR) (of note, values derived from 3D echocardiography and CMR are usually greater than those derived from 2D echocardiography).

When using LA strain to assess diastolic function, elevated LV filling pressure is reflected in reductions in LA reservoir and pump strains (Figure 9C). Recent studies have shown that LA strain has a stronger correlation with invasive LV filling pressure than LAVi.³⁹ There are small age- and sex-related differences in normal values for LA reservoir and pump strains.³⁶ Values for LA reservoir strain < 19–23% are considered abnormally low.

The optimal cut-off to differentiate between normal and elevated LV filling pressures was 18% for LA reservoir strain and 8% for pump strain, when defining PCWP > 12 mmHg as elevated, and 16 and 6%,

respectively, when using PCWP ≥ 15 mmHg as a criterion for elevated filling pressure.³⁹ The association between LA strain and LV filling pressure was strongest in patients with reduced LVEF. In the most recent EACVI consensus document on imaging of patients suspected of HFpEF, it is recommended to include LA reservoir strain as a parameter of LV filling pressure (Figure 6A).

Diastolic stiffness by cardiac shear wave elastography

Increased LV diastolic stiffness is a cardinal feature of HFpEF, but previously, no non-invasive parameter of diastolic stiffness was available.

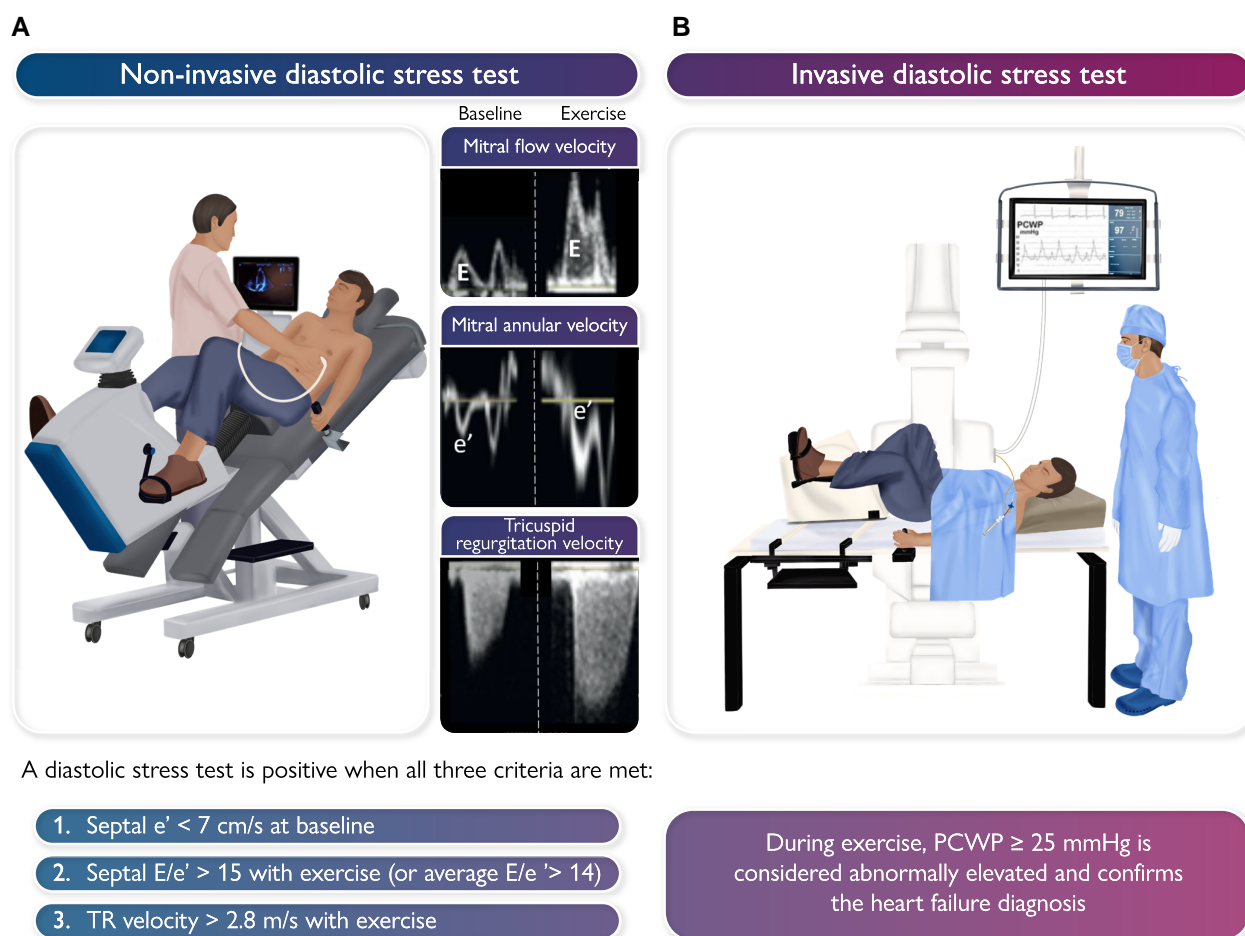


Figure 8 (A) Illustration of a non-invasive diastolic stress test using echocardiography. The inserted traces show mitral flow velocity, mitral annular velocity, and tricuspid regurgitant velocity at rest and during exercise. (B) Illustration of an invasive diastolic stress test with bicycle exercise during right heart catheterization. During the test, PCWP as measure of LV filling pressure is recorded.

Cardiac shear wave elastography was recently proposed as a method to assess LV stiffness.

It is well established that the elastance or stiffness of the myocardium is related to how and at which velocity a shear wave is propagated along the myocardium. With technological advances in echocardiography, it has become possible to image the velocity of the shear wave along the myocardium. The technique is based on high-frame rate shear wave elastography and was introduced very recently in the human heart.⁴¹ The shear wave is based on a tissue displacement perpendicular to the wave propagation direction, which originates from a vibration at the onset region. This vibration can originate naturally upon valve closure—aortic and mitral valves when focusing on the LV—or might be induced mechanically by the probe or another external source.⁴² The shear wave velocity is then calculated from the M-mode along the myocardium from base to apex. When three LV imaging planes are acquired, it is possible to map the shear wave velocity on a LV bull's eye plot (Figure 10).⁴³

There have been several pre-clinical and clinical studies that clearly demonstrate the value of shear wave imaging for the evaluation of myocardial stiffness.⁴³ Nevertheless, shear wave velocity is a surrogate of myocardial stiffness and might be limited by confounding mechanical and/or haemodynamic factors. Therefore, it remains to be studied

the ideal setting for shear wave imaging accounting for these factors. And ultimately, it remains to be studied how shear wave velocity is related to global cardiac stiffness as quantified from the LVEDP–volume relationship.⁴²

Use of echocardiography to differentiate between specific cardiomyopathies

Cardiomyopathy is defined as a myocardial disorder in which the heart muscle is structurally and functionally abnormal in the absence of coronary artery disease, hypertension, valvular disease, and congenital heart disease sufficient to cause the observed myocardial abnormality.⁴⁴ The diagnosis is often challenging, and in many cases, echocardiography does not provide all the diagnostic information needed. Therefore, supplementary imaging by CMR, nuclear techniques, computed tomography (CT), and genetic testing is often needed.

With the introduction of therapies for several cardiomyopathies, it is increasingly important to be aware of echocardiographic features of the different phenotypes, such as amyloidosis, Fabry disease, and glycogen

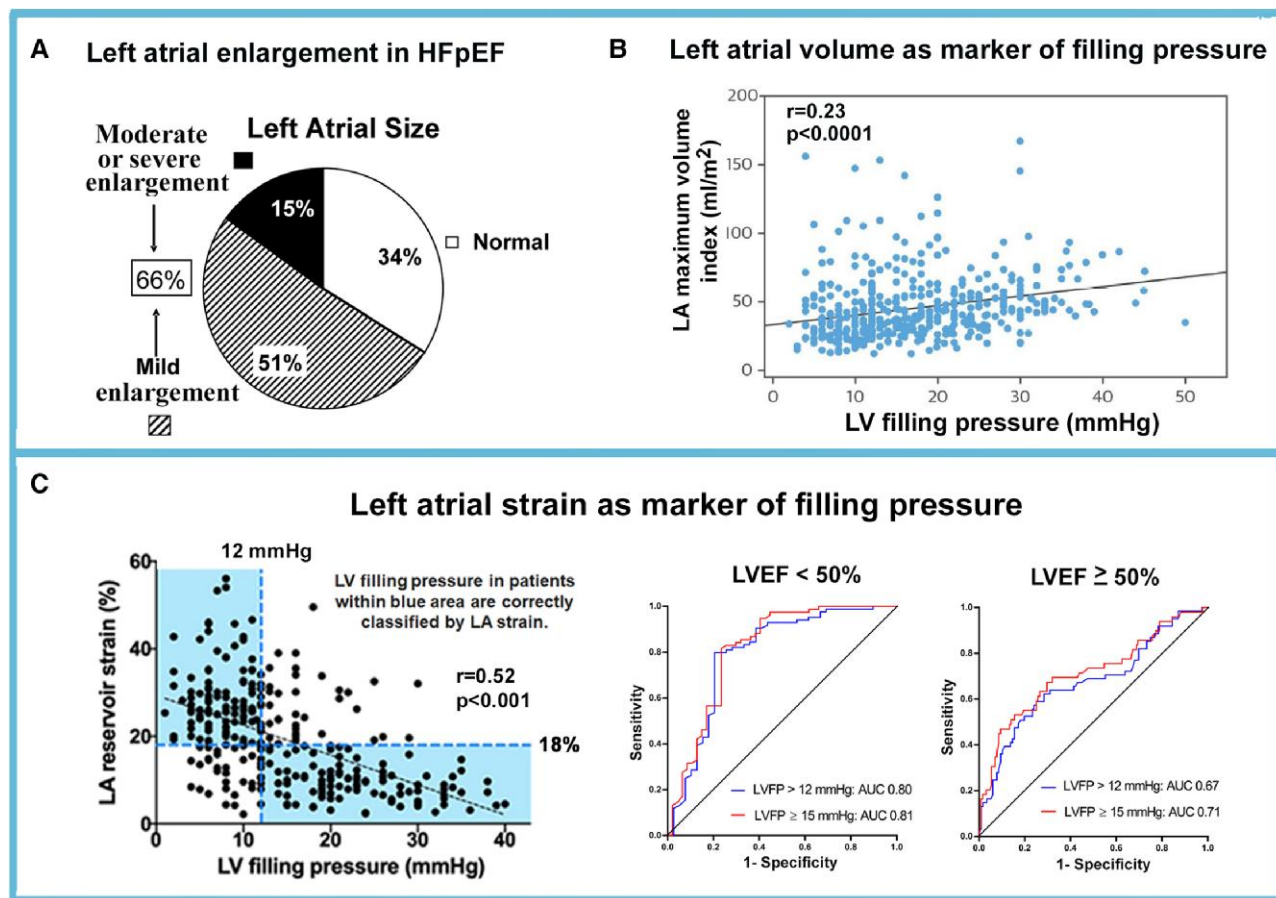


Figure 9 The LA as a biomarker in HF. (A) Prevalence of LA enlargement in HFpEF patients.³⁷ (B) LA volume as a marker of LV filling pressure in patients evaluated for HF. Data from a multicentre study in 450 patients with HF of different aetiologies.³⁸ (C) LA strain as a marker of LV filling pressure. Data from a multicentre study of 322 patients with cardiovascular disease of different aetiologies.³⁹ Left: relationship between LA reservoir strain and LV filling pressure. Right: receiver operating characteristic curves showing the ability of LA reservoir strain to classify LV filling pressure as normal or elevated. Two different definitions of elevated LV filling pressure were used with cut-offs of >12 and ≥15 mmHg. Classification was best in patients with reduced systolic function. Adapted from Inoue et al.³⁹

storage disease, among others. Distribution patterns of segmental myocardial strains may provide diagnostic clues.

Right ventricular function

The presence of right ventricular (RV) dysfunction in HF is strongly associated with increased morbidity and mortality.⁴⁵ Right-sided HF is present when there is evidence of RV dysfunction and signs/symptoms of RV failure.⁴⁶

Echocardiography is the first-line imaging modality used in patients with suspected RV dysfunction and/or pulmonary hypertension. It provides a quantification of right-sided cardiac chamber sizes and function and an estimation of pulmonary arterial systolic pressure (PASP) using the peak tricuspid regurgitation systolic velocity with a cut-off value of >2.8 m/s signifying pulmonary hypertension. RV systolic function is assessed by parameters similar to its counterpart, the LV. These include tricuspid annular plane systolic excursion (TAPSE), fractional area change (FAC), s' , averaged peak longitudinal strain over the three segments of the RV free wall, or global RV strain, which includes both the

free wall and the septum and 3D RVEF. Estimation of right atrial pressure, RV hypertrophy, and septal motion is also performed.

The most frequently used parameter of systolic function is TAPSE with a cut-off value of <17 mm signifying dysfunction followed by FAC, with a cut-off value of <35%. TAPSE and FAC are the most studied parameters with accumulating evidence in relation to prognosis and should preferably be assessed in all patients if possible.^{46,47} RV strain, with a cut-off value of <20% for impaired RV free wall strain (<23% in case of severe tricuspid regurgitation), is angle independent and may detect regional changes when conventional parameters are normal.⁴⁸ It is also less sensitive to tethering effects of the LV, which may influence both TAPSE and s' . 3D RVEF with a cut-off of <45% is an emerging method to quantify systolic function.

Septal position and motion during the cardiac cycle are important in the evaluation of RV dysfunction. Ventricular interdependency is more pronounced in a setting of biventricular failure affecting the septum. In general, septal flattening during systole is associated with RV pressure overload and during diastole with RV volume overload, in both cases an effect of the reduced LV-to-RV transseptal pressure gradient.

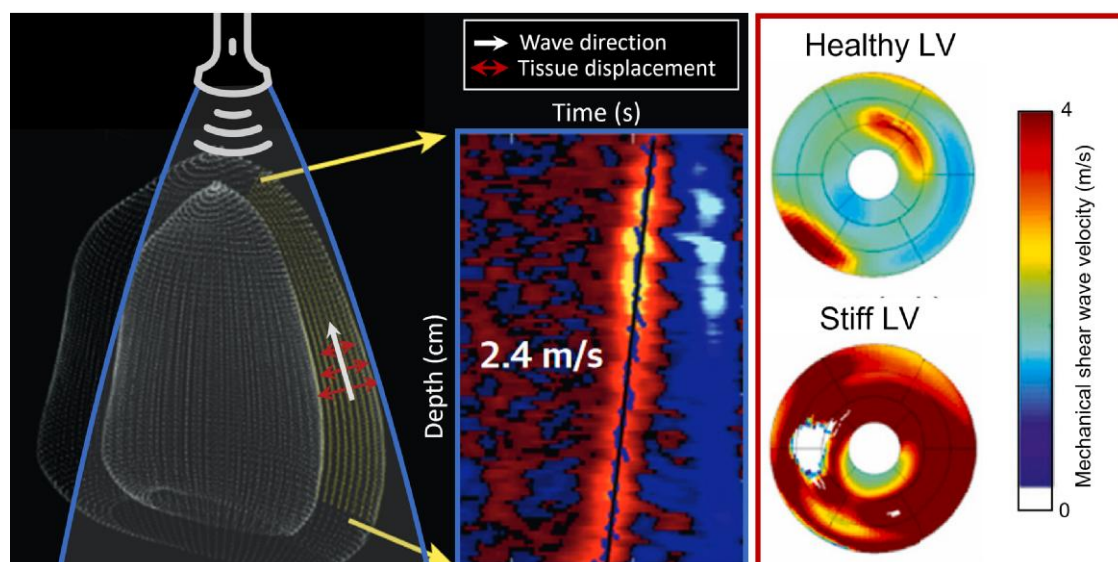


Figure 10 Schematic representation of mechanical shear wave velocity acquisition (left) and example of shear wave mapping for quantifying passive stiffness (right), based on Salles et al.⁴³ High-frame rate M-mode echocardiography along the myocardium captures the tissue displacement acceleration and deceleration originating from mitral valve closure. The slope of the peak displacement over time and over myocardial length gives the shear wave velocity. A stiff myocardium is characterized by a high shear wave velocity. LV, left ventricle.

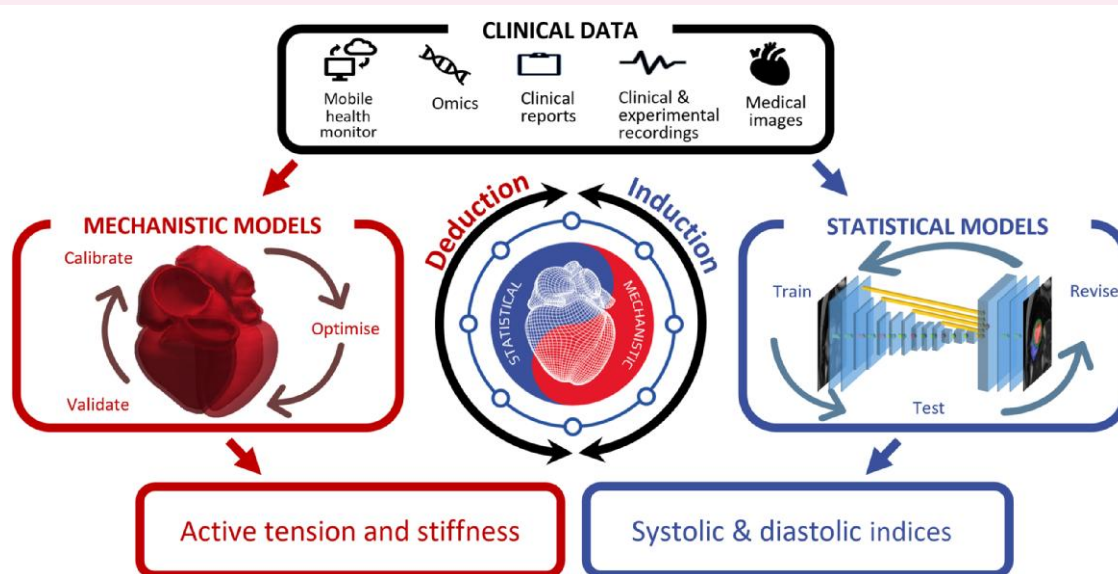


Figure 11 Use of digital twin technologies to extract cardiac functional biomarkers, by either mechanistic models that extract the parameters that rule LV systolic and diastolic function or statistical models that learn from previous examples to rank the disease stage (systolic and diastolic indices).⁵⁰

The RV is sensitive to changes in afterload, and assessment of the interplay between RV contractility and afterload is important. The ratio of end-systolic elastance (Ees) (ventricular contractility) to arterial elastance (Ea) (end-systolic pressure/stroke volume) is obtained invasively and is considered the gold standard of RV–pulmonary arterial coupling. The optimal Ees/Ea is between 1.5

and 2, where a ratio of <0.8–0.6 has been associated with worse outcomes.⁴⁹ Low values of the non-invasive surrogate, the TAPSE/PASP ratio, are associated with worse prognosis in both HFrEF and HFpEF.⁴⁹

When RV images by echocardiography are suboptimal, which occurs especially in obesity and chronic obstructive pulmonary disease,

or a specific diagnosis such as ARVC is suspected, further imaging with CMR is necessary.

A digital twin of systolic and diastolic performance

The ability to build a computational representation of patient-specific LV performance, i.e. its digital twin, offers new opportunities for better management of HF. A digital twin is a model, a simplified representation of reality, which brings a computer-enhanced ability to reason, either through deduction (using mechanistic models) or through induction (using statistic models).⁵⁰

Unveiling the hidden parameters that govern the heartbeat is one of the main values provided by a digital twin (Figure 11). Systole may be simplified into the ability to generate tension by myocytes. And there are two main mechanistic processes that govern filling, the active relaxation of myocytes and the passive storage of strain energy. The quest is then for the extraction of the temporal profile of active tension (generation and relaxation) and the stiffness of the myocardium. The way to estimate these key hidden parameters is the personalization of a mechanical model accounting for the 3D anatomy, material constitutive parameters, and cellular contraction and relaxation.⁵¹

Decaying active tension and myocardial stiffness become the fundamental properties able to dissect out the aetiology of impaired filling. These model-derived biomarkers may provide novel and more specific myocardial diagnostics than global pressure-volume loop-derived chamber stiffness.⁵² There are nevertheless a range of challenges that need careful consideration in the extraction of these LV functional biomarkers.

The first challenge is access to the right data, specifically filling pressure. In fact, one would need the pericardial pressure to get the actual pressure difference that drives diastolic filling. Taking informed guesses of filling pressure, the healthy stiffness of the human myocardium has been estimated at 1.2 ± 0.4 kPa.⁵² Novel methods to estimate filling pressure would be a promising strategy to get these needed data.

The second challenge is the choice of modelling assumptions that are suitable for the question asked and the data available. Cardiac mechanics is a multiscale process spanning through organ, tissue, cell, and ion levels. But the data for each patient are far too limited to personalize models at all those scales. Assumptions for the orientation of fibre bundles for tissue incompressibility or for reference configuration are part of the collection of model choices needed to hit the right level of complexity.^{51,52}

Even at the tissue level, myocardial tissue displays a non-linear behaviour that is difficult to parameterize with the limited range of deformation observed during a heartbeat. In other words, it is difficult to uncouple the linear and exponential parts of the constitutive material behaviour,⁵¹ and previous works mainly aim to estimate the linear one. The choice of metrics that fundamentally remove the interplay, such as energy cost function, is a promising strategy to address it.⁵³

Once the hidden parameters are unveiled, simulations hold the potential to predict long-term effects of concentric or eccentric remodeling. Digital twin technologies also encompass the ability to teach machines how to interpret medical images through statistical models, i.e. machine learning. These models extract the hidden patterns in the data to solve a task and have for example recently been used to extract HF severity via random forest models.⁵⁴ The main challenges here are related to statistical inductive inference, i.e. bounds of generality and robustness and the lack of interpretability or mechanisms that explain the inference.

Although digital twin technology is at an early stage, it holds promise as a future approach for a better understanding of mechanisms of HF and may serve as a means to refine phenotyping.

Funding

None declared.

Conflict of interest: O.A.S. is a co-inventor of 'Method for myocardial segment work analysis' and has received one speaker honorarium from GE Healthcare. O.A.S. and J.F.F. have filed patent on 'Estimation of blood pressure in the heart.'

Data availability

No new data were generated or analysed in support of this research.

References

- McDonagh TA, Metra M, Adamo M, Gardner RS, Baumbach A, Böhm M et al. 2021 ESC guidelines for the diagnosis and treatment of acute and chronic heart failure: developed by the task force for the diagnosis and treatment of acute and chronic heart failure of the European Society of Cardiology (ESC) with the special contribution of the Heart Failure Association (HFA) of the ESC. *Eur Heart J* 2021;**42**:3599–726.
- Wagner S, Cohn K. Heart failure: a proposed definition and classification. *Arch Intern Med* 1977;**137**:675–8.
- Bozkurt B, Coats AJS, Tsutsui H, Abdelhamid M, Adamopoulos S, Albert N et al. Universal definition and classification of heart failure: a report of the Heart Failure Society of America, Heart Failure Association of the European Society of Cardiology, Japanese Heart Failure Society and Writing Committee of the Universal Definition of Heart Failure. *J Card Fail* 2021;**27**:387–413.
- Kraigher-Krainer E, Shah AM, Gupta DK, Santos A, Claggett B, Pieske B et al. Impaired systolic function by strain imaging in heart failure with preserved ejection fraction. *J Am Coll Cardiol* 2014;**63**:447–56.
- Shah KS, Xu H, Matsouka RA, Bhatt DL, Heidenreich PA, Hernandez AF et al. Heart failure with preserved, borderline, and reduced ejection fraction: 5-year outcomes. *J Am Coll Cardiol* 2017;**70**:2476–86.
- Wehner GJ, Jing L, Haggerty CM, Suever JD, Leader JB, Hartzel DN et al. Routinely reported ejection fraction and mortality in clinical practice: where does the nadir of risk lie? *Eur Heart J* 2020;**41**:1249–57.
- Skaarup KG, Lassen MCH, Johansen ND, Sengeløv M, Olsen FJ, Jensen GB et al. Link between myocardial deformation phenotyping using longitudinal and circumferential strain and risk of incident heart failure and cardiovascular death. *Eur Heart J Cardiovasc Imaging* 2023;**24**:999–1006.
- Stokke TM, Hasselberg NE, Smedsrud MK, Sarvari SI, Haugaa KH, Smiseth OA et al. Geometry as a confounder when assessing ventricular systolic function. *J Am Coll Cardiol* 2017;**70**:942–54.
- Farsalinos KE, Daraban AM, Ünlü S, Thomas JD, Badano LP, Voigt JU. Head-to-head comparison of global longitudinal strain measurements among nine different vendors: the EACVI/ASE inter-vendor comparison study. *J Am Soc Echocardiogr* 2015;**28**:1171–1181.e2.
- Haland TF, Hasselberg NE, Almaas VM, Deigaard LA, Saberniak J, Leren IS et al. The systolic paradox in hypertrophic cardiomyopathy. *Open Heart* 2017;**4**:e000571. Available at: <http://openheart.bmj.com/content/4/1/e000571.abstract>
- Smiseth OA, Aalen JM, Skulstad H. Heart failure and systolic function: time to leave diagnostics based on ejection fraction? *Eur Heart J* 2021;**42**:786–8.
- Truong VT, Vo HQ, Ngo TNM, Mazur J, Nguyen TTH, Pham TTM et al. Normal ranges of global left ventricular myocardial work indices in adults: a meta-analysis. *J Am Soc Echocardiogr* 2022;**35**:369–377.e8.
- Sugimoto T, Dulgheru R, Bernard A, Ilardi F, Contu L, Addetia K et al. Echocardiographic reference ranges for normal left ventricular 2D strain: results from the EACVI NORRE study. *Eur Heart J Cardiovasc Imaging* 2017;**18**:833–40.
- Skaarup KG, Lassen MCH, Johansen ND, Olsen FJ, Lind JN, Jørgensen PG et al. Age- and sex-based normal values of layer-specific longitudinal and circumferential strain by speckle tracking echocardiography: the Copenhagen City Heart Study. *Eur Heart J Cardiovasc Imaging* 2022;**23**:629–40. <https://doi.org/10.1093/ehjci/jeab032>.
- Singulane CC, Miyoshi T, Mor-Avi V, Cotella JJ, Schreckenber M, Blankenhagen M et al. Age-, sex-, and race-based normal values for left ventricular circumferential strain from the World Alliance Societies of Echocardiography study. *J Am Soc Echocardiogr* 2023;**36**:581–590.e1.
- Smiseth OA, Torp H, Opdahl A, Haugaa KH, Urheim S. Myocardial strain imaging: how useful is it in clinical decision making? *Eur Heart J* 2016;**37**:1196–207.
- Helle-Valle T, Crosby J, Edvardsen T, Lyseggen E, Amundsen BH, Smith HJ et al. New noninvasive method for assessment of left ventricular rotation. *Circulation* 2005;**112**:3149–56.
- Lang RM, Badano LP, Mor-Avi V, Afilalo J, Armstrong A, Ernande L et al. Recommendations for cardiac chamber quantification by echocardiography in adults: an update from the American Society of Echocardiography and the European Association of Cardiovascular Imaging. *Eur Heart J Cardiovasc Imaging* 2015;**16**:233–71.

19. Russell K, Eriksen M, Aaberge L, Wilhelmsen N, Skulstad H, Remme EW et al. A novel clinical method for quantification of regional left ventricular pressure-strain loop area: a non-invasive index of myocardial work. *Eur Heart J* 2012;**33**:724–33.
20. Smiseth OA, Donal E, Penicka M, Sletten OJ. How to measure left ventricular myocardial work by pressure-strain loops. *Eur Heart J Cardiovasc Imaging* 2021;**22**:259–61.
21. Manganaro R, Marchetta S, Dulgheru R, Ilardi F, Sugimoto T, Robinet S et al. Echocardiographic reference ranges for normal non-invasive myocardial work indices: results from the EACVI NORRE study. *Eur Heart J Cardiovasc Imaging* 2019;**20**:582–90.
22. Chan J, Edwards NFA, Khandheria BK, Shiino K, Sabapathy S, Anderson B et al. A new approach to assess myocardial work by non-invasive left ventricular pressure-strain relations in hypertension and dilated cardiomyopathy. *Eur Heart J Cardiovasc Imaging* 2019;**20**:31–9.
23. Russell K, Eriksen M, Aaberge L, Wilhelmsen N, Skulstad H, Gjesdal O et al. Assessment of wasted myocardial work: a novel method to quantify energy loss due to uncoordinated left ventricular contractions. *Am J Physiol Heart Circ Physiol* 2013;**305**:H996–H1003.
24. Calvillo-Argüelles O, Thampinathan B, Somerset E, Shalmon T, Amir E, Steve Fan CP et al. Diagnostic and prognostic value of myocardial work indices for identification of cancer therapy-related cardiotoxicity. *JACC Cardiovasc Imaging* 2022;**15**:1361–76.
25. Aalen JM, Donal E, Larsen CK, Duchenne J, Lederlin M, Cvijic M et al. Imaging predictors of response to cardiac resynchronization therapy: left ventricular work asymmetry by echocardiography and septal viability by cardiac magnetic resonance. *Eur Heart J* 2020;**41**:3813–23.
26. Anand V, Kane GC, Scott CG, Pislaru S V, Adigun RO, McCully RB et al. Prognostic value of peak stress cardiac power in patients with normal ejection fraction undergoing exercise stress echocardiography. *Eur Heart J* 2021;**42**:776–85.
27. Opdahl A, Remme EW, Helle-Valle T, Lyseggen E, Vartdal T, Pettersen E et al. Determinants of left ventricular early-diastolic lengthening velocity. *Circulation* 2009;**119**:2578–86.
28. Weiss JL, Frederiksen JW, Weisfeldt ML. Hemodynamic determinants of the time-course of fall in canine left ventricular pressure. *J Clin Invest* 1976;**58**:751–60.
29. Smiseth OA, Morris DA, Cardim N, Cikes M, Delgado V, Donal E et al. Multimodality imaging in patients with heart failure and preserved ejection fraction: an expert consensus document of the European Association of Cardiovascular Imaging. *Eur Heart J Cardiovasc Imaging* 2022;**23**:e34–61.
30. Nagueh SF, Smiseth OA, Appleton CP, Byrd BF III, Dokainish H, Edvardsen T et al. Recommendations for the evaluation of left ventricular diastolic function by echocardiography: an update from the American Society of Echocardiography and the European Association of Cardiovascular Imaging. *Eur Heart J Cardiovasc Imaging* 2016;**17**:1321–60.
31. Cheng CP, Noda T, Nozawa T, Little WC. Effect of heart failure on the mechanism of exercise-induced augmentation of mitral valve flow. *Circ Res* 1993;**72**:795–806.
32. Obokata M, Kane GC, Reddy YN V, Olson TP, Melenovsky V, Borlaug BA. Role of diastolic stress testing in the evaluation for heart failure with preserved ejection fraction. *Circulation* 2017;**135**:825–38.
33. Hong SJ, Shim CY, Kim D, Cho JJ, Hong GR, Moon SH et al. Dynamic change in left ventricular apical back rotation: a marker of diastolic suction with exercise. *Eur Heart J Cardiovasc Imaging* 2018;**19**:12–9.
34. Ha JW, Oh JK, Pelikka PA, Ommen SR, Stussy VL, Bailey KR et al. Diastolic stress echocardiography: a novel noninvasive diagnostic test for diastolic dysfunction using supine bicycle exercise Doppler echocardiography. *J Am Soc Echocardiogr* 2005;**18**:63–8.
35. Ha JW, Andersen OS, Smiseth OA. Diastolic stress test: invasive and noninvasive testing. *JACC Cardiovasc Imaging* 2020;**13**(1, Part 2):272–82.
36. Nielsen AB, Skaarup KG, Hauser R, Johansen ND, Lassen MCH, Jensen GB et al. Normal values and reference ranges for left atrial strain by speckle-tracking echocardiography: the Copenhagen City Heart Study. *Eur Heart J Cardiovasc Imaging* 2021;**23**:42–51.
37. Zile MR, Gottdiener JS, Hetzel SJ, McMurray JJ, Komajda M, McKelvie R et al. Prevalence and significance of alterations in cardiac structure and function in patients with heart failure and a preserved ejection fraction. *Circulation* 2011;**124**:2491–501.
38. Andersen OS, Smiseth OA, Dokainish H, Abudiyab MM, Schutt RC, Kumar A et al. Estimating left ventricular filling pressure by echocardiography. *J Am Coll Cardiol* 2017;**69**:1937–48.
39. Inoue K, Khan FH, Remme EW, Ohte N, García-Izquierdo E, Chetrit M et al. Determinants of left atrial reservoir and pump strain and use of atrial strain for evaluation of left ventricular filling pressure. *Eur Heart J Cardiovasc Imaging* 2021;**23**:61–70.
40. Caballero L, Kou S, Dulgheru R, Gonjilashvili N, Athanassopoulos GD, Barone D et al. Echocardiographic reference ranges for normal cardiac Doppler data: results from the NORRE study. *Eur Heart J Cardiovasc Imaging* 2015;**16**:1031–41.
41. Santos P, Petrescu AM, Pedrosa J, Orlowska K, Moini V, Voigt JU et al. Natural shear wave imaging in the human heart: normal values, feasibility, and reproducibility. *IEEE Trans Ultrason Ferroelectr Freq Control* 2019;**66**:442–52.
42. Caenen A, Pernot M, Nightingale KR, Voigt JU, Vos HJ, Segers P et al. Assessing cardiac stiffness using ultrasound shear wave elastography. *Phys Med Biol* 2022;**67**:02TR01.
43. Salles S, Espeland T, Molares A, Aase SA, Hammer TA, Støylen A et al. 3D myocardial mechanical wave measurements: toward in vivo 3D myocardial elasticity mapping. *JACC Cardiovasc Imaging* 2021;**14**:1495–505.
44. Thiene G, Corrado D, Basso C. Revisiting definition and classification of cardiomyopathies in the era of molecular medicine. *Eur Heart J* 2008;**29**:144–6.
45. Ghio S, Gavazzi A, Campana C, Inserra C, Klersy C, Sebastiani R et al. Independent and additive prognostic value of right ventricular systolic function and pulmonary artery pressure in patients with chronic heart failure. *J Am Coll Cardiol* 2001;**37**:183–8.
46. Gorter TM, van Veldhuisen DJ, Bauersachs J, Borlaug BA, Celutkienė J, Coats AJS et al. Right heart dysfunction and failure in heart failure with preserved ejection fraction: mechanisms and management. Position statement on behalf of the Heart Failure Association of the European Society of Cardiology. *Eur J Heart Fail* 2018;**20**:16–37.
47. Burke MA, Katz DH, Beussink L, Selvaraj S, Gupta DK, Fox J et al. Prognostic importance of pathophysiologic markers in patients with heart failure and preserved ejection fraction. *Circ Heart Fail* 2014;**7**:288–99.
48. Morris DA, Krisper M, Nakatani S, Köhncke C, Otsuji Y, Belyavskiy E et al. Normal range and usefulness of right ventricular systolic strain to detect subtle right ventricular systolic abnormalities in patients with heart failure: a multicentre study. *Eur Heart J Cardiovasc Imaging* 2017;**18**:212–23.
49. Houston BA, Brittain EL, Tedford RJ. Right ventricular failure. *N Engl J Med* 2023;**388**:1111–25.
50. Corral-Acero J, Margara F, Marciniak M, Rodero C, Loncaric F, Feng Y et al. The 'digital twin' to enable the vision of precision cardiology. *Eur Heart J* 2020;**41**:4556–64.
51. Xi J, Lamata P, Niederer S, Land S, Shi W, Zhuang X et al. The estimation of patient-specific cardiac diastolic functions from clinical measurements. *Med Image Anal* 2013;**17**:133–46.
52. Wang ZJ, Wang VY, Bradley CP, Nash MP, Young AA, Cao JJ. Left ventricular diastolic myocardial stiffness and end-diastolic myofibre stress in human heart failure using personalised biomechanical analysis. *J Cardiovasc Transl Res* 2018;**11**:346–56.
53. Nasopoulou A, Shetty A, Lee J, Nordsletten D, Rinaldi CA, Lamata P et al. Improved identifiability of myocardial material parameters by an energy-based cost function. *Biomech Model Mechanobiol* 2017;**16**:971–88.
54. Jiang R, Yeung DF, Behnami D, Luong C, Tsang MYC, Jue J et al. A novel continuous left ventricular diastolic function score using machine learning. *J Am Soc Echocardiogr* 2022;**35**:1247–55.